https://doi.org/10.15407/ujpe65.6.510

S. PEREPELYTSYA

Bogolyubov Institute for Theoretical Physics of the Nat. Acad. of Sci. of Ukraine
(14b, Metrolohichna Str., Kyiv 03143, Ukraine; e-mail: perepelytsya@bitp.kiev.ua)

POSITIVELY AND NEGATIVELY HYDRATED COUNTERIONS IN MOLECULAR DYNAMICS SIMULATIONS OF DNA DOUBLE HELIX

The DNA double helix is a polyanionic macromolecule that is neutralized in water solutions by metal ions (counterions). The property of counterions to stabilize the water network (positive hydration) or to make it friable (negative hydration) is important in terms of the physical mechanisms of stabilization of the DNA double helix. In the present research, the effects of positive hydration of Na^+ counterions and negative hydration of K^+ and Cs^+ counterions incorporated into the hydration shell of the DNA double helix have been studied using molecular dynamics simulations. The results have shown that the dynamics of the hydration shell of counterions depends on the region of the double helix: minor groove, major groove, and outside the macromolecule. The longest average residence time has been observed for water molecules contacting with the counterions localized in the minor groove of the double helix (about 50 ps for Na^+ and lower than 10 ps for K^+ and Cs^+). The estimated potentials of the mean force for the hydration shells of counterions show that the water molecules are constrained too strongly, and the effect of negative hydration for K^+ and Cs^+ counterions has not been observed in the simulations. The analysis has shown that the effects of counterion hydration can be described more accurately with water models having lower dipole moments.

K e y w o r d s: DNA, counterion, hydration, residence time, molecular dynamics.

1. Introduction

The DNA macromolecule consists of two polynucleotide chains that, in a water solution, are twisted around each other as a double helix [1]. The key feature of the structure, as discovered in the famous research by James Watson and Francis Crick [2] and supported by X-ray images by Rosalind Franklin [3] and Maurice Wilkins [4], is that the hydrophobic nucleotide bases are localized inside the double helix, minimizing the contacts with water molecules, while the backbone is faced to the solution. The backbone of the double helix comprises the phosphate groups, with each of them having a charge equal to $-1e$. The negatively charged phosphate groups attract the positively charged ions from the solution resulting in the formation of a shell of counterions around the double helix [5–7]. The counterions neutralize the phosphate groups of DNA reducing the electrostatic repulsion of the opposite strands of the double helix. Therefore, water molecules and counterions of the ion-hydration shell around DNA are indispensable for the formation of the double helix and may be considered as the integral part of its structure.

The physical properties of the DNA ion-hydration shell are essentially different from those of bulk water and depend on the region of the double helix: minor groove, major groove, and outside the macromolecule [8–13]. In the minor groove of the double

helix, the mean residence time of a water molecule is the longest (up to 100 ps), while, in the major groove, especially near the phosphate groups, it is several times shorter than in the minor groove of the macromolecule [12, 13]. The counterions can disorder or stabilize the water structure inside the DNA ion-hydration shell. Depending on the structure organization of water molecules, the ions are usually classified into the positively hydrated and the negatively hydrated ones [14]. In the case of positively hydrated ions (Li^+, Na^+, and Mg^{2+}), the water molecules in the hydration shells are highly ordered, and the mean residence time of the molecule in the ion's hydration shell is much longer than that in the bulk solution [14]. Therefore, these ions are also known as the structure-making ions [15]. In the case of negatively hydrated ions (K^+, Rb^+, and Cs^+), the mean residence time of water molecules near the ion is shorter than that in the bulk [14], and the structure of the hydration shell is more friable than that of pure liquid water. Therefore, these ions are also known as the structure-breaking ions [15]. The structure and dynamics of the DNA ion-hydration shell depend on the character of hydration of counterions.

To describe the structure of the ion-hydration shell of the DNA double helix, a theory similar to the statistical theory of electrolytes [16] should be developed. In the present time, the features of the structure of the counterion system around DNA are described within the framework of different theoretical approaches. In particular, the polyelectrolyte models that consider the macromolecule as a chain of charged beads or as a uniformly charged cylinder [17, 18] describe the effect of condensation of counterions observed experimentally [19–22]. On the other hand, considering the structure of DNA with counterions as an ionic-type lattice (ion-phosphate lattice), the vibrations of counterions with respect to the phosphate groups have been found in the low-frequency Raman spectra of DNA (<200 cm^{-1}) [23–28]. The concept of a ion-phosphate lattice has been proven to be useful for describing different effects of the DNA-counterion interaction [29, 30]. The existing theoretical approaches make a general outline of the structural and dynamical properties of the DNA-counterion systems.

In the theoretical descriptions, the water around DNA is usually presented as a continuum with some dielectric constant. At the same time, for the consideration of the hydration effects of counterions, water should be considered explicitly. In this regard, the method of classical molecular dynamics seems the most appropriate. The molecular dynamics studies [11, 31–37] have shown that the counterion distribution around the double helix depends on the sequence of nucleotide bases, region of the double helix, and is governed by the interplay between counterions and water molecules. In particular, the study of the counterion hydration [36] has shown that the structure-making ions interact with DNA mostly via water molecules of the hydration shell, while the structure-breaking ions may squeeze through the DNA hydration shell to the groove bottom and form long-lived complexes with the atoms of nucleotide bases. The difference in the interactions of the structure-making and the structure-breaking counterions with the DNA double helix is explained by different structures and dynamics of the hydration shells of the ions.

The purpose of this research is to study the character of hydration of Na^+, K^+, and Cs^+ counterions incorporated into the hydration shell of the DNA double helix. To solve this problem, the trajectories of atomistic molecular dynamics simulations of DNA with counterions have been analyzed. The radial distribution functions of water molecules with respect to the ions have been built, and the potentials of mean force have been derived. The average residence times of water molecules in the hydration shell of counterions have been estimated. The results have shown that the dynamics of the hydration shells of counterions depend on the region of the double helix, where the ion is localized. The positive character of hydration has been observed for all counterions. The effects of counterion hydration have been shown to be better described with the use of the water models involving lower dipole moments.

2. Materials and Methods

The analysis of the structure and dynamics of the hydration shells of counterions, localized in different regions of the double helix, has been performed through molecular dynamics simulations [36]. The simulations [36] were carried out for the model systems of DNA in water solutions with the counterions. The polynucleotide duplex d(CGCGAATTCGCG) that is known as the Drew–Dickerson dodecamer [9] was used as the model of DNA double helix. This fragment of DNA is

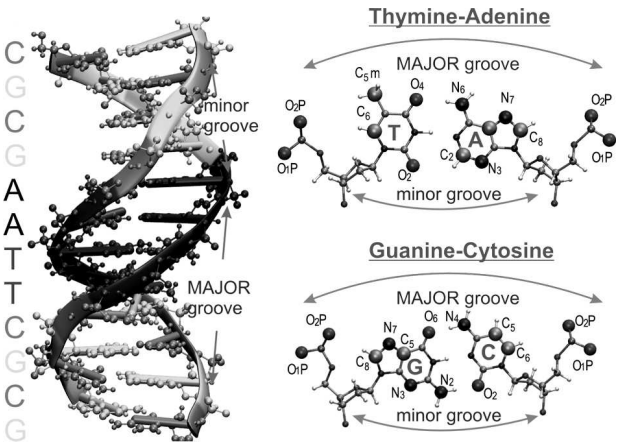

Fig. 1. Structure of the Drew–Dickerson dodecamer d(CGCGAATTCGCG) [9]. The minor and major grooves are indicated. Nucleotide color scheme: Cytosine (orange), Guanine (yellow), Adenine (blue), Thymine (purple) (*a*). Thymine-Adenine and Guanine-Cytosine nucleotide pairs and the reference atoms are shown as enlarged spheres with the names of atoms that were used as reference points for the construction of the radial distribution functions (*b*)

characterized by the narrowed minor groove in the region with AATT nucleotide sequence (Fig. 1, *a*). The major groove is visibly wider comparing to the minor groove. The DNA duplex was immersed into the water box 64×64×64 Å with the metal ions of a definite type: Na^+, K^+ or Cs^+. The number of counterions was 22 that was equal to the number of the DNA phosphate groups, making the system electrically neutral. As a result, three systems of DNA water solutions with the counterions of different types were studied: Na-DNA, K-DNA, and Cs-DNA.

The computer simulations [36] were performed using the NAMD software package [38] and CHARMM27 force field [39, 40]. The length of all bonds with hydrogen atoms was taken rigid using the SHAKE algorithm [41]. The TIP3P water model [42] and the Beglov and Roux parameters of ions have been used [43]. The Langevin dynamics was used for all heavy atoms at a temperature of 300 °K. The total lengths of the simulation trajectory in the NVT ensemble were more than 200 ns for each system. The simulation data were analyzed after 100 ns of the equilibration of the systems. The details of the simulation process are described in [36].

Table 1. **Reference atoms of the DNA macromolecule for the radial distribution functions**

DNA region	Adenine	Guanine	Thymine	Cytosine
Minor groove	N_3, C_2	N_3, N_2	O_2	O_2
Major groove	N_6, C_5, N_7, C_8	O_6, C_5, N_7, C_8	O_4, C_5m, C_6	N_4, C_5, C_6
Phosphates	$PO_{1,2}$	$PO_{1,2}$	$PO_{1,2}$	$PO_{1,2}$

In the present work, the VMD software [44] was used for the analysis and visualization. Using the VMD plug-in [45], the radial distribution functions (RDFs) have been calculated by the following formula:

$$g(r) = p(r)/(4\pi r^2 \Delta r N_p/V), \qquad (1)$$

where $p(r)$ is the average number of atomic pairs found at the distance within $(r \div r + \Delta r)$; N_p is the number of pairs of selected atoms; V is the total volume of the system; Δr is the width of histogram bins which was taken equal to 0.1 Å in the present work. The average number of atomic pairs has been calculated every 10000 time steps that is 500 frames per the nanosecond.

The RDFs have been built for oxygen atoms of water molecules with respect to the ions localized in different regions of the double helix: in the minor and major grooves ($\mathrm{RDF}_{\mathrm{Ion}}^{\mathrm{minor}}$ and $\mathrm{RDF}_{\mathrm{Ion}}^{\mathrm{major}}$), near the phosphate groups ($\mathrm{RDF}_{\mathrm{Ion}}^{ph}$), and in the bulk ($\mathrm{RDF}_{\mathrm{Ion}}^{\mathrm{bulk}}$). The counterion has been considered to be localized in some region of the double helix, if it was within 5 Å of one of the reference atoms. The reference atoms of DNA are shown in Fig. 1, *b* and indicated in Table 1. The same radial distribution functions have been calculated for water molecules with respect to other water molecules localized in different regions of the DNA macromolecule ($\mathrm{RDF}_{W}^{\mathrm{minor}}$, $\mathrm{RDF}_{W}^{\mathrm{major}}$, RDF_{W}^{ph}, and $\mathrm{RDF}_{W}^{\mathrm{bulk}}$). The reference water molecules were not in direct contact with the atoms of the DNA macromolecule.

3. Results

3.1. Radial distribution functions

The obtained radial distribution functions of water molecules with respect to the counterions (ion-water RDFs) are characterized by two maxima: the first is intense and the second is weak (Fig. 2, *a*). The position of maxima are governed by the size of counterion

and water molecule. The intensities of the first and the second maxima depend on a region of the double helix, where the counterion is localized. The only exception was observed in the case of the first maximum for ion-water RDFs of Na^+ counterions that have approximately the same height for all regions of counterion localization. At the same time, in the case of K^+ and Cs^+ counterions, the difference is essential for the first and second maxima.

The RDFs of water molecules with respect to water molecules (water-water RDFs) are characterized by the strong first maximum and a flat curve after (Fig. 2, *b*). The second maximum is very weak and hardly visible. The obtained shapes of the RDFs are characteristic of the TIP3P water model [42, 46]. The difference between water-water RDFs in the case of different regions of the double helix is observed only for the first peak that has always a lower intensity in the case of water molecules in the minor groove.

3.2. Potential of mean force

A water molecule in the hydration shell of an ion is trapped in the potential well and separated from the outer water layer by the potential barrier (Fig. 3). In the present work, the potential barriers for water molecules were estimated with the use of the potentials of mean force (PMF) derived from the radial distribution functions:

$$E(r) = -k_{\mathrm{B}}T \ln\left(g(r)\right), \tag{2}$$

k_{B} is the Boltzmann constant, T is the temperature.

The calculated potentials of mean force are characterized by two potential wells (Fig. 4). In the present work, the dynamics of a water molecule in the first hydration shell is in the scope of interest. Therefore, the first potential well and the potential barrier (ΔE) between the first and second potential wells have been studied.

The results show that the ion-water PMFs have different shapes and depths in the case of different counterions. In the case of Na^+, the potential well is the deepest, whereas, in the case of Cs^+, it is the smallest (Fig. 4, *a*). The difference of ion-water PMFs is also observed for different regions of the double helix, where the counterion may be localized. At the same time, the water-water PMFs are rather similar, and the difference is hardly visible for different regions of the double helix.

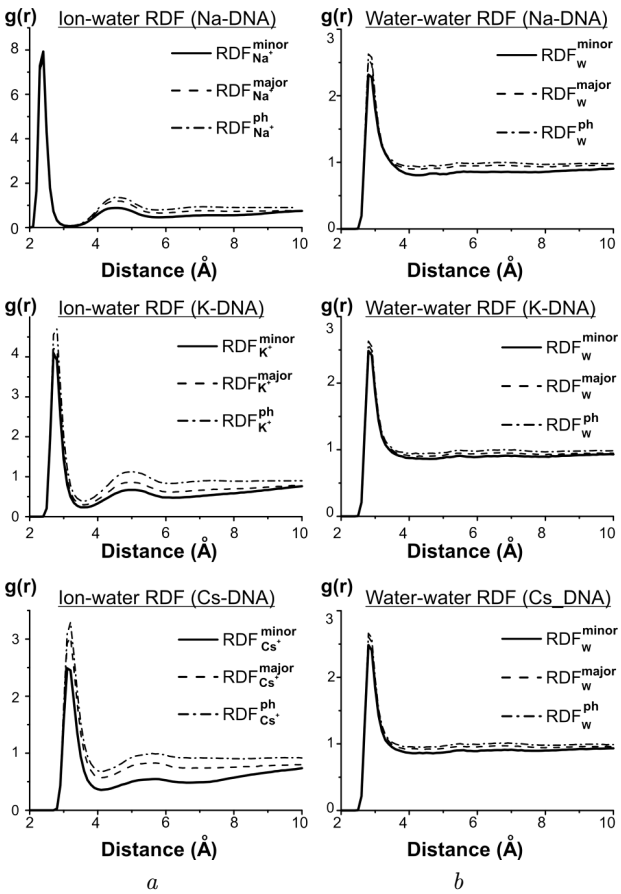

Fig. 2. Radial distribution functions (RDFs) for the oxygen atoms of water molecules with respect to Na^+, K^+, Cs^+ counterions (*a*) and with respect to the other oxygen atoms of water molecules (*b*) in different regions of the double helix: minor groove ($\mathrm{RDF}^{\mathrm{minor}}_{\mathrm{Ion}}$ and $\mathrm{RDF}^{\mathrm{minor}}_{W}$), major groove ($\mathrm{RDF}^{\mathrm{major}}_{\mathrm{Ion}}$ and $\mathrm{RDF}^{\mathrm{major}}_{W}$), and near the phosphate groups of DNA backbone ($\mathrm{RDF}^{ph}_{\mathrm{Ion}}$ and RDF^{ph}_{W})

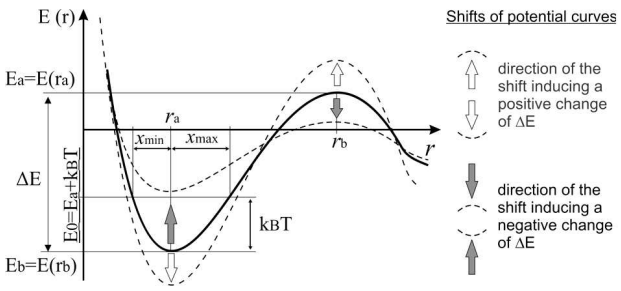

Fig. 3. Schematic structure of the mean field potential energy of a water molecule derived from the radial distribution function. ΔE is the potential energy barrier; E_a and E_b are the energy values in the minimum (r_a) and maximum (r_b), respectively

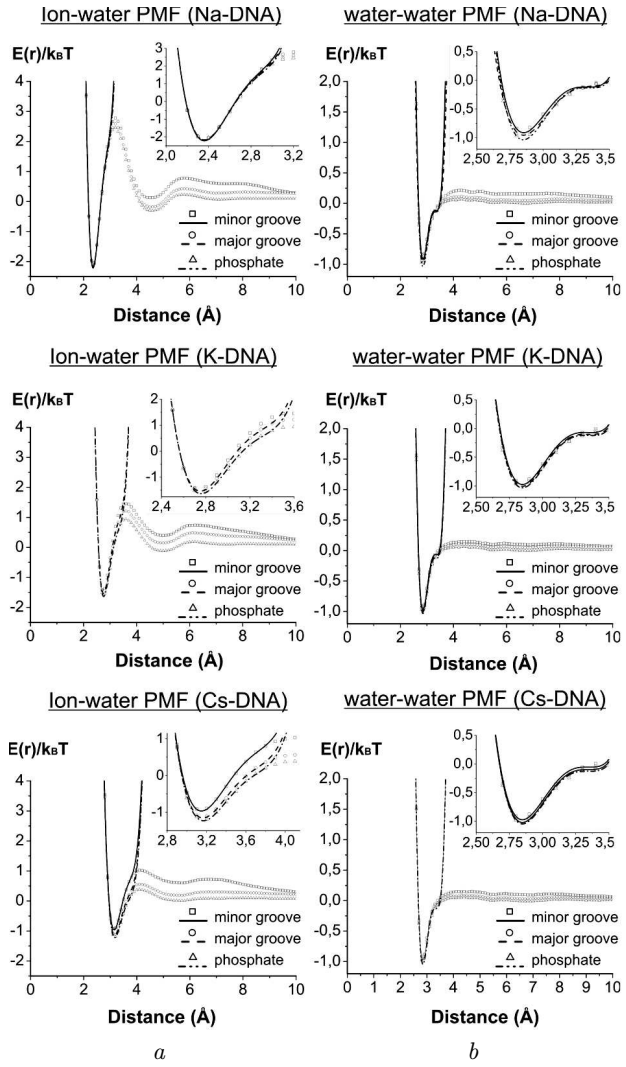

Fig. 4. Potentials of mean force of water molecules (PMFs). The PMFs for water molecules with respect to Na^+, K^+, and Cs^+ in different regions of the double helix (*a*). The PMF for water molecules with respect to the oxygen atoms of water molecules in different regions of the double helix. The lines correspond to curves fitted to PMF: solid, dashed, and dotted lines correspond to the cases of the counterion minor groove, in the major groove, and near the phosphate group of DNA, respectively (*b*)

Using the obtained PMFs, the parameters describing the energy of counterion hydration were calculated by formula (2). The resulted values of the potential barriers for a water molecule in the hydration shell of the ion ($\Delta E_{\rm ion}$) are the highest in the case of Na^+ ions, whereas, in the case of K^+ and Cs^+ ions, the values of $\Delta E_{\rm ion}$ are about two times lower. Such behaviour is a result of different surface charges of the ions due to their different sizes. The energy barrier for a water molecule in the hydration shell of the counterion is much higher than the energy barrier of a water molecule in the bulk ($\Delta E_{\rm ion} > \Delta E_w$). Moreover, in the case of counterions in the minor groove, the potential barrier is the highest, whereas, in the case of a counterion near the phosphate groups and in the bulk, it is much lower (Table 2).

The calculated values of the potential barriers (Table 2) have been compared with the results of molecular dynamics simulations [47] for the ions in aqueous solutions at 25 °C. The values of $\Delta E_{\rm ion}$ for water molecules in the hydration shells of Na^+, K^+, and Cs^+ ions obtained in work [47] are equal to 2.3 kcal/mol, 1.3 kcal/mol, and 0.9 kcal/mol, respectively. Such values are rather close to our results, but, in general, the potential barriers in Table 2 are slightly higher than in work [47]. The reason for different values of $\Delta E_{\rm ion}$ may be related to different water models and ion parameters that have been used in the present work and in work [47].

The difference of the energy barriers for a water molecule in the hydration shell of a counterion and

Table 2. **Parameters of the potentials of mean force. The positions of the minimum and maximum of the potential well r_a and r_b, respectively (in Å). The values of the potential barriers in kcal/mol for water molecules in the hydration shell of the ion ($\Delta E_{\rm ion}$) and for a water molecule surrounded by the other water molecules (ΔE_w)**

System	Na-DNA			K-DNA			Cs-DNA		
Ion-water	r_a	r_b	$\Delta E_{\rm ion}$	r_a	r_b	$\Delta E_{\rm ion}$	r_a	r_b	$\Delta E_{\rm ion}$
Minor gr.	2.36	3.20	3.00	2.75	3.60	1.77	3.15	4.10	1.20
Major gr.	2.36	3.20	2.85	2.75	3.60	1.65	3.16	4.10	1.03
Phosph.	2.36	3.20	2.78	2.75	3.60	1.45	3.17	4.10	0.97
Bulk	2.32	3.15	2.82	2.71	3.55	1.58	3.10	4.05	1.03
Wrater-water	r_a	r_b	$\Delta E_{\rm ion}$	r_a	r_b	$\Delta E_{\rm ion}$	r_a	r_b	$\Delta E_{\rm ion}$
Minor gr.	2.85	4.20	0.68	2.85	4.20	0.67	2.85	4.20	0.68
Major gr.	2.85	4.30	0.64	2.85	4.20	0.67	2.85	4.40	0.66
Phosph.	2.85	4.25	0.67	2.85	4.30	0.66	2.85	4.20	0.66
Bulk	2.79	4.05	0.67	2.84	4.20	0.67	2.84	4.20	0.69

in the bulk ($dE = \Delta E_{\text{ion}} - \Delta E_w$) determines the character of the counterion hydration. The structure-making (positively hydrated) ions have $dE > 0$, while the structure-breaking (negatively hydrated) ions are characterized by $dE < 0$. The obtained results (Table 2) show that the values of dE are positive for all counterions: 2.15 kcal/mol, 0.91 kcal/mol, 0.34 kcal/mol for Na^+, K^+, and Cs^+ counterions, respectively. At the same time, the experimental data [14] show that, among the considered counterions, only a sodium ion has the positive difference of the potential barriers $dE = 0.25$ kcal/mol, and it is much lower than in the simulations. The potassium and cesium ions have a negative difference of the potential barriers $dE = -0.25$ kcal/mol and $dE = -0.33$ kcal/mol, respectively [14]. That is why they are negatively hydrated. The reason for the difference between obtained energy barriers and experimental data may be related to the parametrization of water models that will be discussed in the following section.

3.3. Residence time

The determined potentials of mean force allow us to estimate the residence time τ for water molecules using an equation of the Arrhenius type [14]. In the present work, this equation is presented in the following form:

$$\tau = 2\tau_0 \exp\left(\frac{\Delta E}{k_{\text{B}}T}\right), \tag{3}$$

where τ_0 is the characteristic time for the molecule to approach the potential barrier ΔE. The factor 2 in formula (3) means that the water molecule being at the top of the potential barrier may leave the hydration shell or return back to the potential well with the equal probability. The value of τ_0 is estimated as a period of vibrations of a particle in a potential well using the law of energy conservation for the finite motion [48]:

$$\tau_0 = \sqrt{2\mu} \int\limits_{x_{\min}}^{x_{\max}} \frac{dx}{\sqrt{E_0 - E(x)}}, \tag{4}$$

where μ is the mass of a water molecule; $x = r - r_a$ is the displacement of a water molecule from the equilibrium position r_a; $x_{\min}$ and $x_{\max}$ are the amplitude displacements; E_0 is the amplitude energy of vibrations of a water molecule in the potential well (Fig. 3). The potential function $E(x)$ is determined from the potential of mean force in the approximation of a polynomial function:

$$E(x) \approx E_a + C_2x^2/2 + C_3x^3/3 + C_4x^4/4, \tag{5}$$

where E_a is the depth of the potential well; C_2, C_3, and C_4 are the fitting parameters. The amplitude displacements (x_{min} and $x_{\max}$) were determined from the condition: $E(x) = E_0$ (Fig. 3). Taking Boltzmann's law of equal distribution of energy over degrees of freedom into account, the magnitude of the vibrational amplitude energy was determined as follows: $E_0 = E_a + k_{\text{B}}T$. By substituting (5) to Eq. (4), we obtain the elliptic integral.

The calculated average residence times of water molecules in the hydration shell of an ion are within the range from about 2 ps to 50 ps (Table 3). The longest residence time was observed for the case of sodium counterions, whereas, in the case of potassium and cesium ions, it is several times lower. The dependence of τ values on the region of counterion localization is also observed. The longest residence times of water molecules have been observed for the hydration shells of the ions localized in the minor groove of the double helix (τ_{minor}), whereas, in the major groove (τ_{major}) and near the phosphate group of the macromolecule backbone (τ_{ph}), the residence times are shorter: $\tau_{\text{minor}} > \tau_{\text{major}} > \tau_{ph}$.

Table 3. **Residence times (τ) and the half-period of vibrations (τ_0) in ps for water molecules in the hydration shell of a counterion and for those surrounded by other water molecules**

System	Na-DNA		K-DNA		Cs-DNA	
Ion-water	τ	τ_0	τ	τ_0	τ	τ_0
Minor gr.	52.33	0.18	8.87	0.23	5.02	0.34
Major gr.	41.54	0.18	7.60	0.24	4.29	0.39
Phosph.	37.02	0.18	5.26	0.23	4.10	0.41
Bulk	39.28	0.18	6.51	0.24	4.05	0.36
Water-water	τ	τ_0	τ	τ_0	τ	τ_0
Minor gr.	3.61	0.58	4.22	0.69	4.34	0.71
Major gr.	3.79	0.65	4.19	0.69	4.31	0.72
Phosph.	4.15	0.69	4.23	0.71	4.68	0.85
Bulk	3.25	0.54	3.29	0.54	4.86	0.74

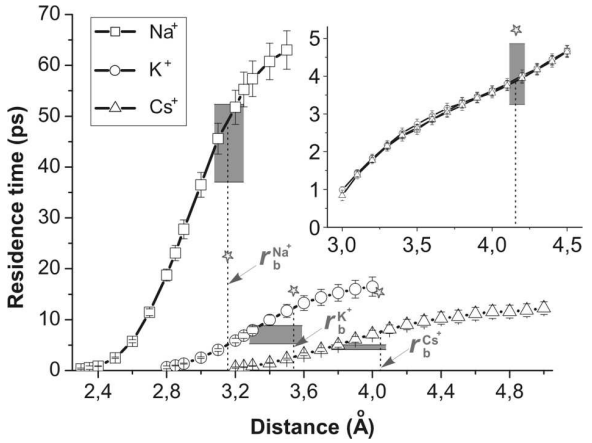

Fig. 5. Dependence of the average residence time of water molecules near Na^+, K^+, and Cs^+ counterions on the distance from the ion. The range of residence times from Table 3 is grayed out. The dotted lines show the distances of RDF minima (r_b) that also correspond to the position of the potential barriers of PMF. Inset: the dependence of the average residence time on the O–O distance for water molecules in the bulk in the case of three simulated systems. The asterisks show the values of the residence times obtained in work [47]

The residence times of water molecules near the counterions have been also calculated using the simulation trajectories. In the analysis, a water molecule was taken into account as a part of the hydration shell of the ion, if the oxygen atom was localized within a distance r_h. The distance r_h characterizes the outer boundary of the hydration shell and should be close to the minimum of the radial distribution function (values of r_b are given in Table 2). The values of the residence times were averaged over all counterions of the system. The obtained values of the residence times increase with the distance r_h (Fig. 5). In the case of Na^+ counterions, the τ values obtained from PMF (Table 3) agree with the values obtained from the analysis of simulation trajectories at the distance $r_h = r_b$ (grey region in Fig. 5). In the case of K^+ and Cs^+ counterions, the values of the residence times calculated by different methods are close at some distance that is lower than r_b. The difference $r_h - r_b$ is less than 0.2 Å, i.e., within the accuracy limit of the estimations. The τ values for water molecules in the bulk (inset in Fig. 5) are in agreement with the calculated values from PMF. Thus, the values of the average residence times of water molecules estimated in the present work by two different methods are in the sufficient agreement.

The obtained average residence times (Table 3) have been compared with the other results of molecular dynamics simulations for alkali metal ions in water solutions [47]. The residence times obtained in work [47] have the same dependence on the ion size as that in the present work, but the absolute τ values are different (asterisks in Fig. 5). There may be several reasons for such disagreement. However, the most essential reason may be the use of different definitions of the residence time and the methods for its calculation. In the present work, the residence time was calculated from the mechanistic approximation of the motion of a water molecule in the potential well that was obtained on the basis of the potential of mean force. In work [47], the residence time was calculated as the integral of the time correlation functions. These methods are not equivalent and the additional analysis should be done to find, where they give the same result.

Thus, the results of molecular dynamics simulations for DNA with the positively hydrated Na^+, and negatively hydrated K^+ and Cs^+ counterions show that the dynamics of water molecules in the hydration shells of counterions depends on their localization around the double helix. In particular, the longest residence time was observed for a water molecule near the counterion that is localized inside the minor groove of the double helix, and it is longer than for the case of a water molecule near the same ion, but in a bulk water. This difference may be due to the confined space inside the double helix and due to the structured system of water molecules that is formed in DNA grooves. At the same time, the results clearly show that the obtained energy barriers for water molecules near the ions are too high, making the hydration shell too rigid. The counterions Na^+, K^+, and Cs^+ in the simulated systems are positively hydrated, and the effect of negative hydration for K^+ and Cs^+ was not observed.

4. Discussion

To explain the reason for high values of the potential barriers, the possible influence of a water model should be analyzed. The TIP3P water model that was used in the simulations is characterized by the dipole moment value 2.35 D, while the experimental values for a water molecule are 1.86 D in the gas phase and 2.95 D in the liquid phase [51]. In this regard, let us analyze the potential barrier as a function of

the dipole moment. For this purpose, the potential of mean force has been estimated as a change of the free energy of a water molecule after its replacement from the hydration shell of the ion to the bulk water:

$$E \equiv \Delta G = \Delta H - T\Delta S + \Delta G_0, \tag{6}$$

where ΔH and $T\Delta S$ are the enthalpy and entropy contributions, and ΔG_0 is some constant part of the free energy change.

The enthalpy contribution is featured mostly by the interaction of a water molecule with the ion. In work [49], the energy of a water molecule near the ion was successfully described by presenting the water molecule as a dipole in the field of the ion. In our model, the repulsion between a water molecule and an ion at small distances is also taken into consideration. As a result, the enthalpy change may be presented as a sum of the average dipole-dipole ($\overline{U_{i-d}(r)}$) and repulsion ($\overline{U_{\rm rep}(r)}$) terms:

$$\Delta H = \overline{U_{i-d}(r)} + \overline{U_{\rm rep}(r)}. \tag{7}$$

Taking into consideration that the direction of a dipole vector in the electric field of the ion is described by the Boltzmann distribution, the average ion-dipole interaction may be presented in the following form:

$$\overline{U_{i-d}\,(r)} = -k_{\rm B}TL(\alpha)\alpha(r), \tag{8}$$

where $L(\alpha) = \coth\alpha - \alpha^{-1}$ is the Langevin function, and

$$\alpha(r) = \frac{1}{k_{\rm B}T}\,\frac{qd}{4\pi\varepsilon\varepsilon_0 r^2}. \tag{9}$$

Here, q is the charge of the ion; ε is the dielectric constant of the media near the ion; ε_0 is the dielectric constant of vacuum; d is the dipole moment of a water molecule.

The repulsion between a water molecule and an ion is described by the potential in the Born–Mayer form that is used in the description of ions in ionic crystals [50] and the DNA ion-phosphate lattice [27]:

$$U_{\rm rep}\,(r) = Ae^{-r/b}, \tag{10}$$

where A and b are the parameters describing the repulsion between the ion and the water molecule as hard cores.

The motions of dipole moments of water molecules around the ion are hindered, and, in general, the molecules are highly oriented due to the electrostatic field. Therefore, the entropy in our model is assumed to increase with the ion-water distance in the same way as the average direction of the water dipole described by the Langevin function $L(\alpha)$. As a result, the change of the entropy is presented as follows:

$$\Delta S = -s_0 L(\alpha), \tag{11}$$

where s_0 is the entropy of a water molecule in the bulk. The parameters A and s_0 can be derived from the condition for maximum and minimum at the distances r_a and r_b: $\frac{d\Delta G}{dr}|_{r=r_a} = 0$, $\frac{d\Delta G}{dr}|_{r=r_b} = 0$.

The energy contribution ΔG_0 is featured by the interaction energy with other water molecules of the system that includes the both enthalpy and entropy contributions. The determination of these contribution is a complex problem and is not necessary for the estimation of the potential barrier height. In the present work, it is determined from the condition $\Delta G(r_c) = 0$; r_c is some point, where the potential of mean force is equal to zero. Taking this into consideration and using Eqs. (6)–(12), the change of the potential of mean force in $k_{\rm B}T$ units can be written in the following form:

$$\widetilde{E}(r) = -L(\alpha)[\alpha(r) + s_0] + Be^{-\frac{r-r_a}{b}} + \Delta g_0, \tag{12}$$

where $\widetilde{E}(r) = E/k_{\rm B}T$, $B = -A/k_{\rm B}T$; $\Delta g_0 = -L(\alpha_c)(\alpha_c + s_0) + Be^{-(r_c-r_a)/b}$, and $\alpha_c = \alpha(r_c)$.

To estimate the energy using formula (12), the parameters have been determined in the following way. The repulsion parameter is taken the same as in the case of the crystals of alkali metal ion that is $b \approx 0.3$ Å [50]. The temperature is taken the same as in the molecular dynamics simulations $T = 300°$ K [42]. The dipole moment $d = 2.35$ D was taken the same as in the TIP3P model of a water molecule. The values of equilibrium distances (r_a) and the barrier distance (r_b) were taken from Table 2. The distance r_c is defined as $r_c = (r_a + r_b)/2$. The dielectric constant has been determined using the dielectric function [52] developed for the description of the electrostatic interactions in nucleic acids: $\varepsilon(\widetilde{r}) = 78 - 77(0.0128\,\widetilde{r}^2 + 0.16\,\widetilde{r} + 1)\,e^{-0.16\,\widetilde{r}}$, where $\widetilde{r}$ is the distance between charges in Å. At the distance about (2÷4) Å, this function gives the value within the range $\varepsilon \approx (1.3 \div 3)$.

The estimations show that the height of the potential barrier $\Delta E = \widetilde{E}(r_b) - \widetilde{E}(r_a)$ decreases as the

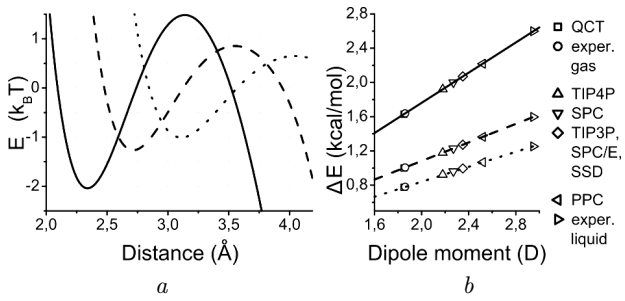

Fig. 6. (*a*) The distance dependence of the energy of a water molecule in the first hydration shell of the ion. (*b*) The dependence of the potential barrier ΔE on the dipole moment of a water molecule. The values of the potential barriers that correspond to the dipole moments of different water models [53–57] and experimental values for a water molecule [51] are shown as the figured points. The lines in (*a*) and (*b*) are made in the solid, dashed, and dotted styles corresponding to Na^+, K^+, and Cs^+ ions, respectively

size of the counterion increases: $\Delta E_{Na^+} > \Delta E_{K^+} > \Delta E_{Cs^+}$ (Fig. 6, *a*). The same dependence of ΔE has been observed in our molecular dynamics simulations (Fig. 4 and Table 2). To analyze the role of the dipole moment of a water molecule, the potential barrier has been calculated using formula (12) for different values of the dipole moment (Fig. 6, *b*). The results show that the potential barrier for a water molecule in the hydration shell of the ion increases linearly with the dipole moment. The values of the potential barriers that correspond to the dipole moments of different water models and experimental data [51, 53–57] (the points in Fig. 6, *b*) are within the range (1.6÷2.6) kcal/mol, (1.0÷1.5) kcal/mol, and (0.7÷1.2) kcal/mol for Na^+, K^+, and Cs^+ ions, respectively. Taking this into consideration, we may conclude that the models of a water molecule with lower dipole moments should give a more accurate description of the hydration effects of counterions.

5. Conclusions

The dynamics of water molecules in the hydration shell of the positively (Na^+) and negatively (K^+ and Cs^+) hydrated counterions around the DNA double helix has been studied. The molecular dynamics simulations for the DNA fragment in a water solution with the counterions at a temperature of 300° K have been used. As a result, the potential barriers and the residence times of water molecules near the counterions have been estimated. The analysis shows that the dynamics of water molecules in the hydration shell of counterions depends on their localization around the double helix that is the manifestation of the interplay between water molecules in the hydration shell of DNA and counterions. The longest residence time of a water molecule has been observed for the case of counterions in the minor groove of the double helix: about 50 ps for Na^+ counterion and less than 10 ps for K^+ and Cs^+ counterions. In the major groove and outside the double helix, it is essentially lower. In the simulations, the counterions constrain water molecules too strongly making the hydration shell more rigid than it should be. As a result, the effect of negative hydration in the case of K^+ and Cs^+ counterion was not obtained. The analysis performed within the framework of the developed phenomenological model shows that the strength of the hydration shell is proportional to the value of the dipole moment in a water model. The water models with lower dipole moments are expected to give a better description of the effects of counterion hydration.

The present work was partially supported by the project of the Department of Physics and Astronomy of the National Academy of Sciences of Ukraine (0117U000240).

1. W. Saenger. *Principles of Nucleic Acid Structure* (Springer, 1984) [ISBN: 978-0471524175].
2. J.D. Watson, F.H.C. Crick. A structure of deoxyribose nucleic acid. *Nature* **171**, 737 (1953).
3. R.E. Franklin, R.G. Gosling. Molecular configuration in sodium thymonucleate. *Nature* **171**, 740 (1953).
4. M.H.F. Wilkins, A.R. Stokes, H.R. Wilson. Molecular structure of deoxypentose nucleic acid. *Nature* **171**, 738 (1953).
5. Yu.P. Blagoy, V.L. Galkin, G.O. Gladchenko *et al. The Complexes of Nucleic Acids with Metal Cations in Solutions* (Naukova Dumka, 1991) (in Russian) [ISBN: 5-12-002499-0].
6. A.V. Sivolob. *Physics of DNA* (Kyiv University, 2011) (in Ukrainian) [ISBN: 978-966-439-468-3].
7. A. Vologodskii, *Biophysics of DNA* (Cambridge Univ. Press, 2015) [ISBN: 9781139542371].
8. V.Ya. Maleev, M.A. Semenov, M.A. Gassan, V.I. Kashpur. Physical properties of the DNA-water system. *Biofizika* **38**, 768 (1993) (in Russian).
9. H.R. Drew, R.M. Wing, T. Takano, C. Broka, S. Takana, K. Itakura, R.E. Dickerson. Structure of a B-DNA dodecamer: Conformation and dynamics. *Proc. Natl. Acad. Sci. USA* **78**, 2179 (1981).

10. V. Tereshko, G. Minasov, M. Egli. A "hydrat-ion" spine in a B-DNA minor groove *J. Am. Chem. Soc.* **121**, 3590 (1999).
11. F. Mocci, A. Laaksonen. Insights into nucleic acid counterion interactions from inside molecular dynamics simulation is "worth its salt". *Soft Matter* **8**, 9268 (2012).
12. D. Laage,T. Elsaesser, J.T. Hynes. Water dynamics in the hydration shells of biomolecules. *Chem. Rev.* **117**, 10694 (2017).
13. E. Duboué-Dijon, A.C. Fogarty, J.T. Hynes, D. Laage. Dynamical disorder in the DNA hydration shell. *J. Am. Chem. Soc.* **138**, 7610 (2016).
14. N.A. Ismailov. *Electro Chemistry of Solutions* (Chemistry, 1976) (in Russian).
15. P.R. Smirnov, V.N. Trostin. Structures of the nearest surroundings of the K^+, Rb^+, and Cs^+ ions in aqueous solutions of their salts. *Russian J. of General Chemistry* **77** (12), 2101 (2007).
16. I.R. Yukhnovskii, M.F. Golovko. *Statistical Theory of Classical Equilibrium Systems* (Naukova Dumka, 1980) (in Russian).
17. G.S. Manning. The molecular theory of polyelectrolyte solutions with applications to the electrostatic properties of polynucleotides. *Quarterly Reviews of Biophysics* **11**, 179 (1978).
18. M.D. Frank-Kamenetskii, V.V. Anshelevich, A.V. Lukashin. Polyelectrolyte model of DNA. *Soviet Physics Uspekhi* **30**, 317 (1987).
19. R. Das, T.T. Mills, L.W. Kwok, G.S. Maskel, I.S. Millett, S. Doniach, K.D. Finkelstein, D. Herschlag, L. Pollack. Counterion distribution around DNA probed by solution X-ray scattering. *Phys. Rev. Lett.* **90**, 188103 (2003).
20. K. Andersen, R. Das, H.Y. Park, H. Smith, L.W. Kwok, J.S. Lamb, E.J. Kirkland, D. Herschlag, K.D. Finkelstein, L. Pollack. Spatial distribution of competing ions around DNA in solution. *Phys. Rev. Lett.* **93**, 248103 (2004).
21. K. Andresen, X. Qiu, S.A. Pabit, J.S. Lamb, H.Y. Park, L.W. Kwok, L. Pollack. Mono- and trivalent ions around DNA: A small-angle scattering study of competition and interactions. *Biophys. J.* **95**, 287 (2008).
22. X. Qiu, K. Andresen, J.S. Lamb, L.W. Kwok, L. Pollack. Abrupt transition from a free, repulsive to a condensed, attractive DNA phase, induced by multivalent polyamine cations. *Phys. Rev. Lett.* **101**, 228101 (2008).
23. S.M. Perepelytsya, S.N. Volkov. Ion mode in the DNA low-frequency vibration spectra. *Ukr. J. Phys.* **49**, 1074 (2004).
24. S.M. Perepelytsya, S.N. Volkov. Counterion vibrations in the DNA low-frequency spectra. *Eur. Phys. J. E* **24**, 261 (2007).
25. L.A. Bulavin, S.N. Volkov, S.Yu. Kutovy, S.M. Perepelytsya. Observation of the DNA ion-phosphate vibrations. *Rep. Nat. Acad. Sci. of Ukraine* No. 11, 69 (2007).
26. S.M. Perepelytsya, S.N. Volkov. Intensities of DNA ion-phosphate modes in the low-frequency Raman spectra. *Eur. Phys. J. E* **31**, 201 (2010).
27. S.M. Perepelytsya, S.N. Volkov. Conformational vibrations of ionic lattice in DNA: Manifestation in the low-frequency Raman spectra. *J. Mol. Liq.* **5**, 1182 (2011).
28. S.M. Perepelytsya, S.N. Volkov. Vibrations of ordered counterions around left-and right-handed DNA double helixes. *J. Phys.: Conf. Ser.* **438**, 012013 (2013).
29. S.M. Perepelytsya, G.M. Glibitskiy, S.N. Volkov. Texture formation in DNA films with alkali metal chlorides. *Biopolymers* **99**, 508 (2013).
30. O.O. Liubysh, O.M. Alekseev, S.Yu. Tkachov, S.M. Perepelytsya. Effect of ionic ordering in conductivity experiments of DNA aqueous solutions. *Ukr. J. Phys.* **59**, 2071 (2014).
31. F. Mocci, G. Saba. Molecular dynamics simulations of A. T-rich oligomers: sequence-specific binding of Na^+ in the minor groove of B-DNA. *Biopolymers* **68**, 471 (2003).
32. R. Lavery, J.H. Maddocks, M. Pasi, K. Zakrzewska. Analyzing ion distribution around DNA. *Nucleic Acids Res.* **42**, 8138 (2014).
33. M. Pasi, J.H. Maddocks, R. Lavery. Analyzing ion distributions around DNA: sequence-dependence of potassium ion distributions from microsecond molecular dynamics. *Nucleic Acids Res.* **43**, 2412 (2015).
34. O.O. Liubysh, A.V. Vlasiuk, S.M. Perepelytsya. Structuring of counterions around DNA double helix: a molecular dynamics study. *Ukr. J. Phys.* **49**, 1074 (2015).
35. A. Atzori, S. Liggi, A. Laaksonen, M. Porcu, A.P. Lyubartsev, G. Saba, F. Mocci. Base sequence specificity of counterion binding to DNA: what can MD simulations tell us? *Canadian J. of Chemistry* **94** (12), 1181 (2016).
36. S. Perepelytsya. Hydration of counterions interacting with DNA double helix: a molecular dynamics study. *J. Mol. Mod.* **24**, 171 (2018).
37. S. Perepelytsya, J. Uličný, A. Laaksonen, F. Mocci. Pattern preferences of DNA nucleotide motifs by polyamines putrescine^{2+}, spermidine^{3+} and spermine^{4+}. *Nucleic Acids Res.* **47**, 6084 (2019).
38. J.C. Phillips, R. Braun, W. Wang, J. Gumbart, E. Tajkhorshid, E. Villa, C. Chipot, R.D. Skeel, L. Kale, K. Schulten. Scalable molecular dynamics with NAMD *J. Comp. Chem.* **26**, 1781 (2005).
39. N. Foloppe, A.D. MacKerell, jr. All-atom empirical force field for nucleic acids: I. Parameter optimization based on small molecule and condensed phase macromolecular target data. *J. Comp. Chem.* **21**, 86 (2000).
40. A.D. MacKerell, jr., N. Banavali. All-atom empirical force field for nucleic acids: II. Application to molecular dynamics simulations of DNA and RNA in solution. *J. Comp. Chem.* **21**, 105 (2000).
41. J.P. Ryckaert, G. Ciccotti, H.J.C. Berendsen. Numerical integration of the Cartesian equations of motion of a system with constraints: molecular dynamics of n-alkanes. *J. Comp. Chem.* **32**, 327 (1977).
42. W.L. Jorgensen, J. Chandrasekhar, J.D. Madura, R.W. Impey, M.L. Klein. Comparison of simple potential

functions for simulating liguids. *J. Chem. Phys.* **79**, 926 (1983).
43. D. Beglov, B. Roux. Finite Representation of an infinite bulk system: solvent boundary potential for computer simulations. *J. Chem. Phys.* **100**, 9050 (1994).
44. W. Humphrey, A. Dalke, K. Schulten. VMD – Visual Molecular Dynamics. *J. Molec. Graphics* **14.1**, 33 (1996).
45. B.G. Levine, J.E. Stone, A. Kolhmeyer. Fast analysis of molecular dynamics trajectories with graphics processing units – radial distribution function hystogramming. *J. Comp. Phys.* **230**, 3556 (2011).
46. M. Pekka, N. Lennart. Structure and dynamics of TIP3P, SPC, and SPC/E water models at 298 K. *J. Phys. Chem. A* **105**, 9954 (2001).
47. S. Koneshan, J.C. Rasaiah, R.M. Lynden-Bell, S.H. Lee. Solvent structure, dynamics, and ion mobility in aqueous solutions at 25 °C. *J. Phys. Chem. B* **102**, 4193 (1998).
48. L.D. Landau, E.M. Lifshitz. *Mechanics* (Butterworth-Heinemann, 2001).
49. V.N. Byakov, V.G. Petukhov, A.M. Sukhanovskaya, V.G. Firsov. *Behavior of Solvation Shell Molecules in an Alternating Electric Field*. Preprint ITEP-52 (ITEP, 1985) (in Russian).
50. C. Kittel. *Introduction to Solid State Physics* (Wiley, 1954) [ISBN: 978-0-471-41526-85].
51. A.V. Gubskaya, P.G. Kusalik. The total molecular dipole moment for liquid water. *J. Chem. Phys.* **117**, 5290 (2002).
52. J. Ramstein, R. Lavery. Energetic coupling between DNA bending and base pair opening. *Proc. Natl. Acad. Sci. USA* **85**, 7231 (1988).
53. S.Y. Liem, P.L.A. Popelier, M. Leslie. Simulation of liquid water using a high-rank quantum topological electrostatic potential. *International J. of Quantum Chem.* **99**, 685 (2004).
54. P.G. Kusalik, I.M. Svishchev. The spatial structure in liquid water. *Science* **265**, 1219 (1994).
55. H.J.C. Berendsen, J.R. Grigera, T.P. Straatsma. The missing term in effective pair potentials. *J. Phys. Chem.* **91**, 6269 (1987).
56. M-L. Tan, J.T. Fischer, A. Chandra, B.R. Brooks, T. Ichiye. A temperature of maximum density in soft sticky dipole water. *Chem. Phys. Lett.* **376**, 646 (2003).
57. K. Kiyohara, K.E. Gubbins, A.Z. Panagiotopoulos. Phase coexistence properties of polarizable water models. *Mol. Phys.* **94**, 803 (1998).

Received 20.12.19

С.М. Перепелиця

ДОДАТНО І ВІД'ЄМНО ГІДРАТОВАНІ ПРОТИІОНИ В МОДЕЛЮВАННІ ПОДВІЙНОЇ СПІРАЛІ ДНК МЕТОДОМ МОЛЕКУЛЯРНОЇ ДИНАМІКИ

Р е з ю м е

Подвійна спіраль ДНК – це поліаніонна макромолекула, яка у водних розчинах нейтралізується іонами металів (протиіонами). Властивість протиіонів стабілізувати структуру води (позитивна гідратація) або робити її розупорядкованою (негативна гідратація) важлива з точки зору фізичних механізмів стабілізації подвійної спіралі ДНК. У даному дослідженні ефекти позитивної гідратації протиіонів Na^+ та негативної гідратації протиіонів K^+ і Cs^+, що вбудовано в гідратну оболонку подвійної спіралі ДНК, вивчалися за допомогою моделювання методом молекулярної динаміки. Результати показали, що динаміка гідратної оболонки протиіонів залежить від області подвійної спіралі: мінорний жолоб, головний жолоб і область ззовні макромолекули. Найдовший середній час перебування спостерігався для молекул води, що контактують з протиіонами, локалізованими у мінорному жолобі подвійної спіралі (приблизно 50 пс для Na^+, і менше 10 пс для K^+ і Cs^+). Розраховані потенціали середньої сили для гідратних оболонок протиіонів показують, що молекули води зв'язані занадто сильно, і ефект негативної гідратації для протиіонів K^+ і Cs^+ в симуляціях не спостерігався. Аналіз показав, що ефекти гідратації протиіонів можна більш точно описати за допомогою моделей молекул води, що мають нижчі значення дипольного моменту.